Raman scattering spectra of coupled LO-phonon-plasmon modes in N-In codoped *p*-type ZnO thin films

J. F. Kong, H. Chen, H. B. Ye, and W. Z. Shen[a)]
Laboratory of Condensed Matter Spectroscopy and Opto-Electronic Physics, Department of Physics, Shanghai Jiao Tong University, 1954 Hua Shan Road, Shanghai 200030, People's Republic of China

J. L. Zhao and X. M. Li
State Key Laboratory of High Performance Ceramics and Superfine Microstructures, Shanghai Institute of Ceramics, Chinese Academy of Sciences, 1295 Ding Xi Road, Shanghai 200050, People's Republic of China

(Received 29 September 2006; accepted 18 December 2006; published online 23 January 2007)

The authors report on a detailed Raman study of N–In codoped *p*-type ZnO thin films with the hole density ranging from 7.30×10^{16} to 2.30×10^{18} cm^{-3}. In addition to the identification of E_2(high) modes of ZnO and InN at ~434 and ~488 cm^{-1}, respectively, clear coupled longitudinal-optical phonon-hole-plasmon modes have been observed. A theoretical analysis combining the deformation potential and electro-optic mechanisms can well reproduce the line shapes of the coupled modes, where the yielded hole densities and mobilities are found to be in good agreement with the data from Hall measurements. © *2007 American Institute of Physics*. [DOI: 10.1063/1.2432955]

In polar semiconductors, the longitudinal-optical (LO) phonons interact with the free-carrier plasmon via their macroscopic electric fields.[1,2] The coupled LO-phonon-plasmon modes (CPPMs) from such interactions were discussed theoretically by Varga[1] and observed experimentally in Raman scattering of *n*-type GaAs by Mooradian and Wright.[3] Since then studies about the CPPMs in various semiconductors have been extensively reported from both experimental and theoretical viewpoints.[2–5] Many CPPM relevant theoretical models have been established to study *n*- and *p*-type semiconductors, where useful carrier transport information has been extracted from the Raman spectrum analysis.

ZnO has attracted considerable interest as a promising material for blue and ultraviolet (UV) light emitting devices, photodetectors, optically gated switches, chemical sensors, and nanomanipulators due to its superior physical properties of a direct wide band gap (3.36 eV), large binding energy (60 meV) at room temperature, and piezoelectricity.[6,7] Recent research interest is focused on the fabrication of *p*-type ZnO to get rid of the growth difficulties such as the self-compensation effect, deep acceptor level, and low solubility of the acceptor dopants.[8] Many groups have reported the growth of *p*-type ZnO, using group-I elements (Li, Cu, and Ag) for Zn sites[9–11] or group-V elements (N, P, and As) for O sites.[12–14] Several groups have also proposed the codoping technique using both acceptors (e.g., N) and donors (e.g., Al, Ga, or In).[8,15,16] Nevertheless, it is worth noting that the carrier transport information of *p*-ZnO is generally extracted from the Hall measurements. One would suspect the reliability of high Hall mobility (~10^1–10^2 cm^2/V s) in the *p*-type ZnO films, since they exhibit high resistivity in most cases.[16] Few studies are available in the literature on the powerful Raman scattering for carrier transport parameters of *p*-type ZnO thin films, in contrast to the comprehensive investigation of the CPPMs in *n*-type ZnO.[4,17,18]

N–In codoped *p*-ZnO thin films were grown by ultrasonic spray pyrolysis method at atmosphere.[8] Intrinsic crystalline Si (*c*-Si) (100) were used as the substrates, which were etched by diluted HF (10%) for 3 min prior to the deposition. The aerosol of precursor solution was generated by the commercial ultrasonic nebulizer and transported to the substrate heated at 450 °C. The atomic ratio of Zn/N/In was 1:3:0.05 in the precursor solution, and the different doping concentrations in the N–In codoped films were realized by the change of the deposition rate. Room-temperature Raman scattering spectra from 330 to 700 cm^{-1} were excited by the UV (325 nm) line of a He–Cd laser, and measured by a Jobin Yvon LabRAM HR 800UV micro-Raman system. Electrical properties of the same samples were characterized by the magnetic field dependent (0–0.6 T) Hall measurements at room temperature.

Figure 1 shows the experimental Raman spectra for six N–In codoped *p*-ZnO thin films with different hole densities where the contributions of the strong ZnO emission have been subtracted from the measured Raman spectra by using base lines in the relevant software of the micro-Raman system. The curves were recorded in a backscattering geometry of $z(x,-)\bar{z}$ configuration, where E_2(high), LO phonon, and CPPM Raman scattering are allowed via deformation potential mechanism.[20] In the case of low hole density in Fig. 1(a), we observe one broad band centered at ~ 440 cm^{-1} and one sharp peak at ~570 cm^{-1}. As the hole density increases, an additional peak centered at ~488 cm^{-1} occurs [see Figs. 1(b)–1(f)]. The full width at half maximum (FWHM) of the peak at ~488 cm^{-1} clearly broadens and its intensity relative to the mode at ~570 cm^{-1} enhances with the hole density [see Fig. 2(a)]. The mode at ~570 cm^{-1} slightly redshifts and its FWHM also broadens with increasing hole density.

In order to identify the above different Raman modes, we have decomposed the experimental Raman spectra into three modes: one Lorentzian mode centered at 434 cm^{-1}, another Lorentzian at ~ 488 cm^{-1}, and the third mode at ~570 cm^{-1} calculated by the *p*-type CPPM theory,[19] which will be discussed in detail below. The first mode centered at 434 cm^{-1} can be attributed to the characteristic nonpolar E_2(high) mode of the wurtzite structure of ZnO.[21] In contrast to the observation in many literatures that the ZnO nonpolar

[a)]Author to whom correspondence should be addressed; electronic mail: wzshen@sjtu.edu.cn

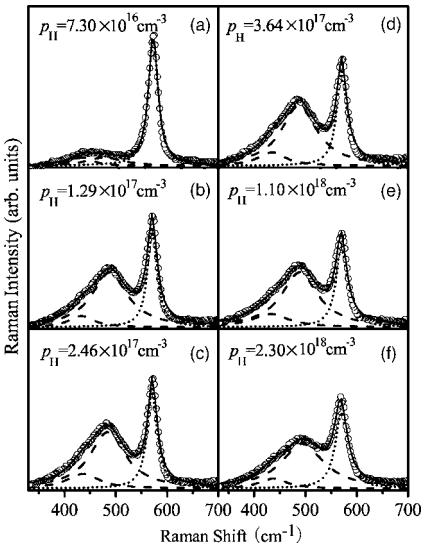

FIG. 1. Room-temperature experimental (open circles) and calculated (solid curves: total fits, and dashed curves: Lorentzian fits, and dotted curves: the CPPM theory fits) Raman spectra of N–In codoped *p*-type ZnO thin films. Photoluminescence backgrounds have been subtracted from the Raman spectra.

E_2(high) mode was almost imperceptible when using a 325 nm (3.8 eV) UV laser, our Raman fitting reveals that it does contribute to the Raman spectra and is independent of the hole density, since the experimental data cannot be well reproduced using the CPPM at ~570 cm^{-1} and only one Lorentzian at ~488 cm^{-1}.

We have attributed the second mode centered at ~488 cm^{-1} to E_2(high) mode of InN based on the following arguments: By using $\omega_{\mathrm{LVM}}=\omega_{\mathrm{ZnO}}[\mu_{\mathrm{ZnO}}/\mu_{\mathrm{LVM}}]^{1/2}$, with μ the effective masses, we obtained the frequencies of 458 and 569 cm^{-1} for local vibrational modes (LVMs) of N on substitutional Zn and O sites in the ZnO lattice, respectively, with the ZnO E_2(high) frequency ω_{ZnO} of 434 cm^{-1}.[21] The calculated frequencies of LVMs for the N–O and N–Zn pairs are also not consistent with the experimental value of 488 cm^{-1}, which indicates that this additional mode is not likely to be the N-related LVM. In fact, the In–N bond in these N–In codoped *p*-ZnO films was observed by x-ray photoelectron spectroscopy measurements,[8] and the E_2(high) phonon mode of InN was located at ~490 cm^{-1}.[22] Further experimental evidence of this assignment comes from the observation that the relative intensity $I(E_2)_{\mathrm{InN}}/I(\mathrm{CPPM})_{\mathrm{ZnO}}$

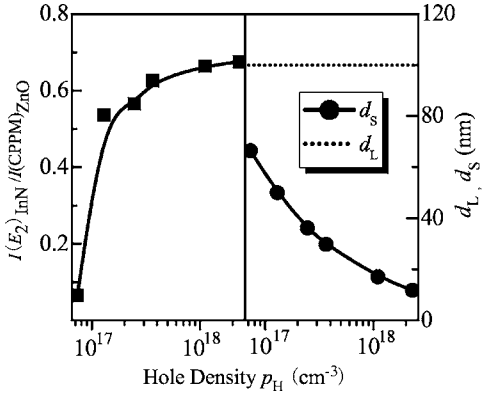

FIG. 2. (a) Intensity ratios $I(E_2)_{\mathrm{InN}}/I(\mathrm{CPPM})_{\mathrm{ZnO}}$ (filled squares) of the InN E_2(high) mode to the ZnO CPPM as a function of Hall density p_H. (b) Depletion layer depth d_S (filled circles) under different Hall densities p_H. The dashed line is the penetration depth d_L of the 325 nm UV laser in ZnO.

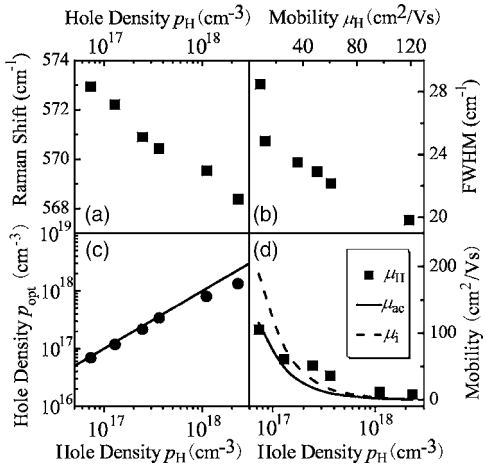

FIG. 3. (a) Raman shift of the ZnO CPPM vs Hall density p_H. (b) FWHM of the ZnO CPPM vs Hall mobility μ_H. (c) Optical hole densities p_{opt} vs Hall density p_H. The solid line represents $p_{\mathrm{opt}}=p_H$. (d) Optical mobilities μ_{ac} (solid curve) and μ_i (dashed curve) compared with μ_H (filled squares).

shown in Fig. 2(a) clearly increases with the hole density, which implies that more and more N and In atoms are codoped into ZnO.

We now focus on the third mode at ~570 cm^{-1}. The penetration depth d_L of the laser light with a wavelength of 325 nm is about 100 nm for ZnO,[23] which is much smaller than the thickness of these N–In codoped *p*-type ZnO films (~300–400 nm). So the mode around 570 cm^{-1} cannot originate from the film-substrate interface. Moreover, Inushima *et al.*[24] have proposed the presence of a depletion layer at the sample surface. The experimental Raman peaks at ~570 cm^{-1} may be ascribed to the contribution of the unscreened LO phonon in the surface depletion layer. Assuming that the film hole density p_H is equal to the density of ionized impurities N_i, the thickness of the surface depletion layer d_S can be estimated through $d_S=(\varepsilon_0\phi/2\pi e^2N_i)^{1/2}$, with ε_0 and ϕ the static dielectric constant and barrier height of the surface potential for *p*-type ZnO, respectively. Since ϕ of *p*-type ZnO is not available, we simply employ the relevant value of *p*-type $Zn_{0.9}Mg_{0.1}O$ (i.e., 0.55–0.56 eV).[25] Figure 2(b) shows the calculated d_S for ZnO with different hole densities using ε_0=7.9. It is clear that the surface depletion layer thickness is always smaller than d_L, excluding the unscreened LO phonon origin of the third Raman mode. It is expected from the CPPM theory that only one CPPM appears in the large damping condition and this CPPM will redshift and broaden with the increase of hole density. We do observe the slight redshift and broadening of the ~570 cm^{-1} structure with increasing hole density/decreasing mobility in Figs. 3(a) and 3(b), clearly indicating that this mode comes from the CPPM in the bulk region of these ZnO thin films.

Since Raman scattering in depolarized geometry is driven by the deformation potential and electro-optic mechanisms, we resort to the CPPM theory proposed by Katayama and Murase[19] for modeling the Raman line shape (I_A), which can be expressed as

$$I_A \propto \mathrm{Im}\left\{\frac{1}{\varepsilon}\left[C^2A^2\chi_{\mathrm{ph}}(\varepsilon_\infty+4\pi\chi_{\mathrm{fc}})-2CA\varepsilon_\infty\chi_{\mathrm{ph}}-\frac{\varepsilon_\infty^2}{4\pi}\right]\right\}, \tag{1a}$$

where C is the Faust-Henry coefficient, $A=\omega_{\mathrm{TO}}^2/(\omega_{\mathrm{LO}}^2-\omega_{\mathrm{TO}}^2)$, and the total dielectric function ε for the phonon and free-carrier system is given by

$$\varepsilon = \varepsilon_\infty + 4\pi\chi_{\rm ph} + 4\pi\chi_{\rm fc} = \varepsilon_\infty\left[1 + \frac{\omega_{\rm LO}^2 - \omega_{\rm TO}^2}{\omega_{\rm TO}^2 - \omega^2 - i\omega\Gamma} - \frac{\omega_p^2}{\omega(\omega + i\gamma)}\right], \quad (1b)$$

with the hole plasma frequency ω_p and the high frequency dielectric constant ε_∞. $\chi_{\rm ph}$ is the free-carrier susceptibility, $\chi_{\rm fc}$ is the ionic susceptibility, $\omega_{\rm LO}$ and $\omega_{\rm TO}$ are the longitudinal and transverse optical frequencies, Γ is the phonon damping constant, and γ is the plasmon damping constant. To calculate the CPPM line shape, we employ $\omega_{\rm LO}=574$ cm^{-1}, $\omega_{\rm TO}=380$ cm^{-1}, $\varepsilon_\infty=3.70$,[26,27] and take ω_p, γ, Γ, and C as adjustable parameters. The final theoretical Raman spectra (Fig. 1) combining the above CPPM and two Lorentzian modes (centered at ~434 and 488 cm^{-1}) are in good agreement with the experimental data. During the CPPM fitting, we find $C=-0.68$ for all the six p-type ZnO samples. It should be pointed out that only one CPPM can be evidenced in the Raman spectra primarily due to the overdamped plasma ($\omega_p \ll \gamma$) in these ZnO films. Similar phenomenon has also been observed in p-type GaN with the hole density in the range of 3×10^{17}–3×10^{18} cm^{-3}.[28]

In addition to the traditional Hall measurements, the above detailed line shape analysis for the CPPM at ~570 cm^{-1} provides us an independent way to extract the transport parameters in p-ZnO thin films. The comparison of these two methods can be further performed to check the reliability of the obtained transport characteristics within the films. The hole density from the optical Raman technique $p_{\rm opt}$ can be directly derived from ω_p through

$$\omega_p^2 = 4\pi p_{\rm opt} e^2/\varepsilon_\infty m_h^*, \quad (2)$$

with $m_h^*=0.59m_0$ the effective mass of the free hole in ZnO.[27] The filled circles in Fig. 3(c) represent the yielded optical density $p_{\rm opt}$ versus the hole density p_H deduced from the Hall measurements. The coincidence between these two techniques is clearly revealed by the fact that the filled circles lie on the solid line of $p_{\rm opt}=p_H$. Due to the complex valence-band structure, the effective Hall coefficient is likely to differ from unity, while this coefficient is still taken as unity in the Hall measurements,[29] resulting in the small deviation between $p_{\rm opt}$ and p_H at high hole densities (above 1.0×10^{18} cm^{-3}).

As for the mobility from the Raman spectrum analysis, we can use the relation[5]

$$m^*\gamma = \frac{3\pi}{8}\frac{e}{\mu_{\rm ac}} \quad (3a)$$

to deduce the acoustic-phonon scattering dominant mobility $\mu_{\rm ac}$. Alternatively, another equation of

$$m^*\gamma = \frac{315\pi}{512}\frac{e}{\mu_i} \quad (3b)$$

is utilized to obtain the ionized-impurity scattering dominant mobility μ_i.[5] Figure 3(d) shows the resultant $\mu_{\rm ac}$ and μ_i, together with the Hall mobility μ_H as a function of Hall density p_H. It is evident from Fig. 3(d) that $\mu_{\rm ac}$ agrees well with μ_H at low hole densities, while μ_i is closely comparable to μ_H at high densities. These can be well understood as follows: The acoustic-phonon scattering is dominant and the ionized-impurity scattering is negligible at low hole densities, while it is the opposite case at high hole densities. In the case of medium hole densities (1.5×10^{17}–1.0×10^{18} cm^{-3}), the mobility of these ZnO films should be a trade-off between phonon and impurity scatterings to some extent. The above good agreement between Raman and Hall measurements on the hole density and mobility clearly demonstrates the reliability of high Hall mobility (~10^1–10^2 cm^2/V s) in the present p-type ZnO thin films.

This work is supported in part by the National Natural Science Foundation of China and the National Minister of Education Program for Changjiang Scholars and Innovative Research Team in University (PCSIRT).

[1] B. B. Varga, Phys. Rev. **137**, A1896 (1965).
[2] R. Fukasawa and S. Perkowitz, Phys. Rev. B **50**, 14119 (1994).
[3] A. Mooradian and G. B. Wright, Phys. Rev. Lett. **16**, 999 (1966).
[4] B. H. Bairamov, A. Heinrich, G. Irmer, V. V. Toporov, and E. Ziegler, Phys. Status Solidi B **119**, 227 (1983).
[5] H. Yugami, S. Nakashima, and A. Mitsuishi, J. Appl. Phys. **61**, 354 (1987).
[6] M. H. Huang, S. Mao, H. Feick, H. Q. Yan, Y. Y. Wu, H. Kind, E. Weber, R. Russo, and P. D. Yang, Science **292**, 1897 (2001).
[7] H. Chik, J. Liang, S. G. Cloutier, N. Kouklin, and J. M. Xu, Appl. Phys. Lett. **84**, 3376 (2004).
[8] J. M. Bian, X. M. Li, X. D. Gao, W. D. Yu, and L. D. Chen, Appl. Phys. Lett. **84**, 541 (2004).
[9] A. Valentini, F. Quaranta, M. Rossi, and G. Battaglin, J. Vac. Sci. Technol. A **9**, 286 (1991).
[10] Y. Kanai, Jpn. J. Appl. Phys., Jpn. J. Appl. Phys., Part 1 **30**, 703 (1991).
[11] Y. Kanai, Jpn. J. Appl. Phys., Jpn. J. Appl. Phys., Part 1 **30**, 2021 (1991).
[12] T. Aoki, Y. Hatanaka, and D. C. Look, Appl. Phys. Lett. **76**, 3257 (2000).
[13] D. C. Look, D. C. Reynolds, C. W. Litton, R. L. Jones, D. B. Eason, and G. Cantwell, Appl. Phys. Lett. **81**, 1830 (2002).
[14] Y. R. Ryu, T. S. Lee, and H. W. White, Appl. Phys. Lett. **83**, 87 (2003).
[15] M. Joseph, H. Tabata, and T. Kawai, Jpn. J. Appl. Phys., Part 2 **38**, L1205 (1999).
[16] Z. Z. Ye, F. Z. Ge, J. G. Lu, Z. H. Zhang, L. P. Zhu, B. H. Zhao, and J. Y. Huang, J. Cryst. Growth **265**, 127 (2004).
[17] M. Göppert, F. Gehbauer, M. Hetterich, J. Münzel, D. Queck, and C. Klingshirn, J. Lumin. **72-74**, 430 (1997).
[18] E. A. Kafadaryan, S. I. Petrosyan, A. G. Hayrapetyan, R. K. Hovsepyan, A. L. Manukyan, and E. S. Vardanyan, J. Appl. Phys. **95**, 3005 (2000).
[19] S. Katayama and K. Murase, J. Phys. Soc. Jpn. **42**, 886 (1977).
[20] R. Cuscó, J. Ibáñez, and L. Artús, Phys. Rev. B **57**, 12197 (1998).
[21] G. T. Du, Y. Ma, Y. T. Zhang, and T. P. Yang, Appl. Phys. Lett. **87**, 213103 (2005).
[22] X. D. Pu, J. Chen, W. Z. Shen, H. Ogawa, and Q. X. Guo, J. Appl. Phys. **98**, 033527 (2005).
[23] V. Srikant and D. R. Clarkea, J. Appl. Phys. **81**, 6357 (1997).
[24] T. Inushima, T. Shiraishi, and V. Y. Davydov, Solid State Commun. **110**, 491 (1999).
[25] S. Kim, B. S. Kang, F. Ren, Y. W. Heo, K. Ip, D. P. Norton, and S. J. Peartona, Appl. Phys. Lett. **84**, 1904 (2004).
[26] T. C. Damen, S. P. S. Porto, and B. Tell, Phys. Rev. **142**, 570 (1966).
[27] W. R. L. Lambrecht, A. V. Rodina, S. Limpijumnong, B. Segall, and B. K. Meyer, Phys. Rev. B **65**, 075207 (2002).
[28] F. Demangeot, J. Frandon, M. A. Renucci, N. Grandjean, B. Beaumont, J. Massies, and P. Gibart, Solid State Commun. **106**, 491 (1998).
[29] H. J. Lee and D. C. Look, J. Appl. Phys. **54**, 4446 (1983).